

# Post Print

## Low-energy d-d excitations in MnO studied by resonant x-ray fluorescence spectroscopy

S. M. Butorin, J.-H. Guo, Martin Magnuson, P. Kuiper and J. Nordgren

N.B.: When citing this work, cite the original article.

Original Publication:

S. M. Butorin, J.-H. Guo, Martin Magnuson, P. Kuiper and J. Nordgren, Low-energy d-d excitations in MnO studied by resonant x-ray fluorescence spectroscopy, 1996, Physical Review B. Condensed Matter and Materials Physics, (54), 4405-4408.

<http://dx.doi.org/10.1103/PhysRevB.54.4405>

Copyright: American Physical Society

<http://www.aps.org/>

Postprint available at: Linköping University Electronic Press

<http://urn.kb.se/resolve?urn=urn:nbn:se:liu:diva-17475>

## Low-energy $d-d$ excitations in MnO studied by resonant x-ray fluorescence spectroscopy

S. M. Butorin,\* J.-H. Guo, M. Magnuson, P. Kuiper, and J. Nordgren  
*Department of Physics, Uppsala University, Box 530, S-751 21 Uppsala, Sweden*  
 (Received 10 April 1996)

We measured the Mn  $L_{\alpha,\beta}$  x-ray fluorescence spectra of MnO excited by selected photon energies near the  $L_{2,3}$  absorption edges. The resulting resonant inelastic x-ray scattering spectra probe low-lying electronic excited states, due to  $dd$  and charge-transfer excitations. Using a two-step model and a purely atomic approximation, we reproduce both energies and varying intensities of  $dd$  excitations relative to the electronic recombination peak. Our results show that strongly varying line shapes in resonant x-ray emission need not be due to channel interference effects. [S0163-1829(96)04528-6]

The new, bright sources of x rays make possible experiments like inelastic x-ray scattering spectroscopy. Many kinds of neutral excitations can be probed, from core-level absorption edges<sup>1</sup> down to meV sound excitations in water.<sup>2</sup> With the excitation energy set just above a core-absorption threshold, features in the intense valence x-ray emission spectrum coincide with the x-ray loss peaks due to neutral electronic excitations, enhancing them element specifically by several orders of magnitude. Multichannel interference<sup>3</sup> between close-lying vibrational states or quasidegenerate core-level orbitals<sup>4</sup> can cause strong variations of line shapes in molecules and semiconductors.<sup>5</sup> However, interference is not always the cause of strong line shape changes, as will be shown here.

We apply resonant x-ray fluorescence to the study of  $dd$  excitations in the transition metal compound MnO. These excitations with energies on the order of 1 eV play an important role even at thermal energies: The antiferromagnetic order in MnO is related to the ligand field,<sup>6</sup> high- $T_c$  superconductivity in cuprates may involve  $dd$  excitations on the Cu atoms, and the ligand-field excitations of transition metal ions in some biological enzymes play an important role in their chemical activity. An important goal of various core-hole spectroscopies is to obtain knowledge about the ground state and low-energy excited states, but the presence of a core hole complicates analysis of the data. However, it is not easy to study neutral electronic excitations directly. The  $dd$  excitations in transition metal compounds are dipole forbidden and therefore very faint in optical spectroscopy. These excitations can be studied with electron energy loss spectroscopy (EELS) because the dipole selection rules are relaxed at low electron energies,<sup>7</sup> but these measurements are very surface sensitive.

We will present data and calculations to show that resonant x-ray fluorescence is a very promising probe of  $dd$  excitations in transition metal oxides. We will see that a description in two incoherent steps (x-ray absorption followed by emission) describes the process rather well. The first step produces core-hole states in the  $L_{2,3}$  x-ray absorption spectrum. The second step is the decay of the intermediate state, either to the ground state (the electronic recombination peak) or to a different state of the electronic multiplet without a core hole (the loss structures). Because there are two dipole transitions involved, the final state has the same parity as the

initial state, and  $dd$  excitations are not forbidden. The spin-orbit coupling of the  $2p$  orbital allows spin-flip excitations. We will show that the intensities of the loss features can be more easily calculated than the  $dd$  intensities in optical spectroscopy or in EELS. The resolution of our data is far superior to those in an early publication.<sup>8</sup> At present the resolution is still limited by the trade-off against count rate and statistics, but even brighter synchrotron sources will reveal even finer details.

This paper is devoted to  $dd$  excitations but in MnO there are also charge-transfer excitations, transitions involving the transfer of an electron from the ligand  $O^{2-}$  band to the metal ion. These features can be identified in the spectra, though we will not attempt to reproduce them in our model calculations. The application of resonant x-ray fluorescence spectroscopy to studies of charge-transfer excitations is discussed in a paper on Ce  $4f$ -to- $3d$  transitions in  $CeO_2$  and  $CeF_3$ .<sup>9</sup>

The measurements were carried out at beam line 7.0 of the Advanced Light Source, Lawrence Berkeley Laboratory with a spherical grating monochromator.<sup>10</sup> The Mn  $L_{\alpha,\beta}$  x-ray fluorescence spectra of a MnO single crystal were recorded using a grazing-incidence grating spectrometer<sup>11</sup> with a two-dimensional detector. The spectrometer resolution was set to about 0.5 eV. The incidence angle of the photon beam was about 20° to the sample surface and the spectrometer was placed in the horizontal plane at an angle of 90° with respect to the incidence beam. The Mn  $L_{\alpha,\beta}$  emission lines of pure metal<sup>12</sup> were used for energy calibration. To determine the excitation energies, absorption spectra of MnO at the Mn  $2p$  edge were obtained by measuring total electron yield. During x-ray absorption and emission measurements, the resolution of the monochromator was set to about 0.4 eV and 1.5 eV, respectively.

Figure 1 shows the resonant Mn  $L_{\alpha,\beta}$  x-ray fluorescence spectra of MnO, at a number of energies marked in the x-ray absorption spectrum of Fig. 1 (inset) by tics. A spectrum excited far above the edge, producing the normal  $L_{\alpha,\beta}$  emission spectrum, is also shown. These resonant fluorescence spectra reveal much more structure than earlier lower-resolution measurements on MnO,<sup>8</sup> and the relative intensities of all spectral features depend strongly on the excitation energy in a complicated way.

The starting point of the analysis is the x-ray absorption spectrum shown in the inset of Fig. 1. It agrees with previous

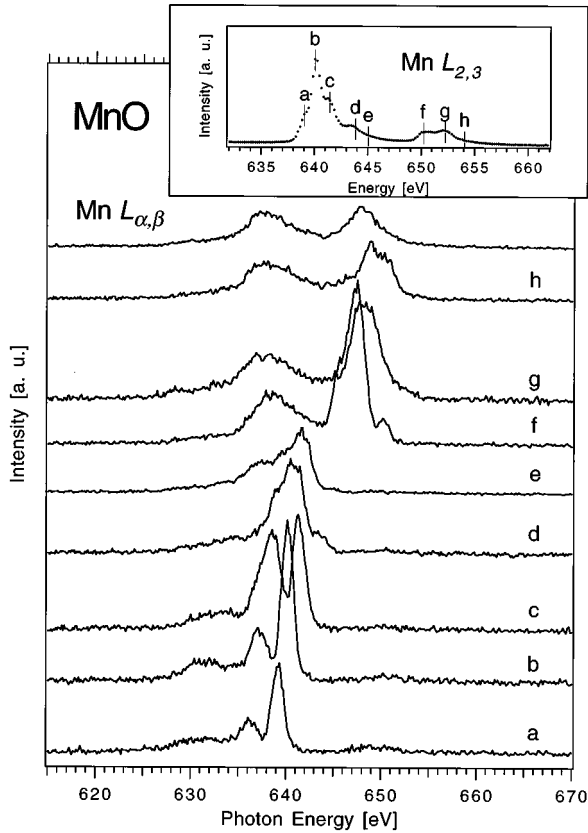


FIG. 1. The Mn  $L_{\alpha,\beta}$  x-ray fluorescence spectra of MnO recorded at different excitation energies near the Mn  $2p$  threshold. The letters correspond to the excitation energies indicated in the absorption spectrum shown in the inset. The excitation for uppermost spectrum was 716 eV.

measurements,<sup>13,14</sup> and is well understood in terms of atomic  $3d^5 \rightarrow 2p^5 3d^6$  transitions in a crystal field.<sup>14,15</sup> The spectrum is dominated by strong multiplet effects due to the Coulomb and exchange interactions between a  $2p$  core hole and  $3d$  electrons in the final states. The large spin-orbit interaction of the  $2p$  hole splits the final states into the  $L_3$  and  $L_2$  groups, approximately 11 eV apart. Although  $2p$  x-ray absorption spectra of  $3d$  compounds are influenced by the crystal field interaction,<sup>16</sup> this dependence is much smaller in  $d^5$  ions than in  $d^4$  or  $d^6$  ions because of the  ${}^6S$  spherical ground state, so that the spectrum of MnO resembles that of Mn vapor.<sup>17</sup>

We can order the fluorescence data by assigning the peaks to one of three categories: the recombination peak, the resonating loss structures due to  $dd$  excitations and charge transfer transitions, and the normal  $L_{\alpha,\beta}$  x-ray emission lines. The electronic recombination peak is at the same energy as the excitation energy, except for the possibility of phonon losses. The width of this peak (approximately 1.5 eV in the first three spectra) is due to a combination of the resolution of the monochromator, the spectrometer, and the absorption profile. The strength of the recombination peak shows that the excited electron stays bound to the core hole as an exciton. From Fig. 1 it is clear that the relative intensity of the recombination peak decreases with increasing excitation energy. This can be understood as a consequence of the spin ordering of the excited states. The lowest  $2p^5 3d^6$  intermedi-

ate states would have the highest possible spin (also sextuplets). If these states decay, they are likely to end up again as a sextuplet, the  ${}^6S$  ground state, contributing to the recombination line. But at higher energies in the  $L_3$  multiplet one finds quartets and doublets (spin is not conserved because of the large  $2p$  spin-orbit interaction). These higher-lying quartets are less likely to recombine into the sextuplet ground state, which explains the relatively weak recombination line. This general ordering of the spin states in the intermediate state is not only true within the  $L_3$  region, but also over the whole spectrum, as explained by Thole and van der Laan.<sup>18</sup> Within the  $L_2$  region, we see a clearly lower intensity of the elastic peak on the high-energy slope (Fig. 1, spectra  $h$ ) than on the first maximum (Fig. 1, spectra  $f$ ). Another qualitative explanation for the trends in the intensity of the elastic peak is that if the absorption is relatively weak, the optical matrix element from the excited state back to the ground state is also small, and the core hole is more likely to decay to an excited final state.

More interesting than the varying intensity of the recombination peak is the strong dependence on the excitation energy of the rest of the emission spectrum. The spectra consist of resonant and nonresonant parts which can be easily identified. The resonant part follows the excitation energy due to energy conservation since the emitted photon energy  $\omega$  must increase with increasing incident photon energy  $\Omega$  in accordance with the equation  $\Omega + E_g = \omega + E_f$ , where  $E_g$  and  $E_f$  are the energy of the ground ( $|g\rangle$ ) and final ( $|f\rangle$ ) states of the emission process. This gives rise to loss features with a constant difference in energy below the recombination line. The nonresonant fluorescence features appear at the constant energies of emitted photons. Also here energy is conserved, of course, but the excess energy is taken up by the photoelectron in the continuum of band states.

When we plot the resonant x-ray emission spectra as energy loss spectra (Fig. 2), it is easier to identify some of the excitations in the final state. The lowest one around 3 eV is derived from the  ${}^4G$  atomic state that lies 3.13 eV above the ground state according to gas phase data of the neutral atom.<sup>19</sup> An EELS experiment on MnO (Ref. 20) shows the  ${}^4G$  peak at 2.8 eV, with a shoulder at 2.2 eV due to the crystal field splitting of this state. In our data the splitting is just on the edge of being resolved. The spectra  $d$  and  $e$  clearly show a shoulder at 5 eV, which was assigned to the  ${}^4P$  state in the EELS study.<sup>20</sup>

The success of these qualitative explanations of experimental spectra recorded at different excitation energies calls for an attempt to calculate these spectra. If the x-ray fluorescence process is treated as an incoherent optical process, the x-ray fluorescence intensity is given as

$$I(\Omega, \omega) = \sum_f \sum_i \frac{| \langle f | r_q | i \rangle \langle i | r_q | g \rangle |^2}{(E_i - E_g - \Omega)^2 + \Gamma^2} \delta(E_f + \omega - E_g - \Omega), \quad (1)$$

where  $|i\rangle$  is an intermediate state with energy  $E_i$  and lifetime broadening  $\Gamma$  (assumed to be 0.4 eV) and  $r_q$  is the dipole operator. To account for the finite spread of the excitation energy (a monochromator function) and experimental broadening from the spectrometer the calculated spectrum is convoluted with the Gaussian function. The incoherent approach

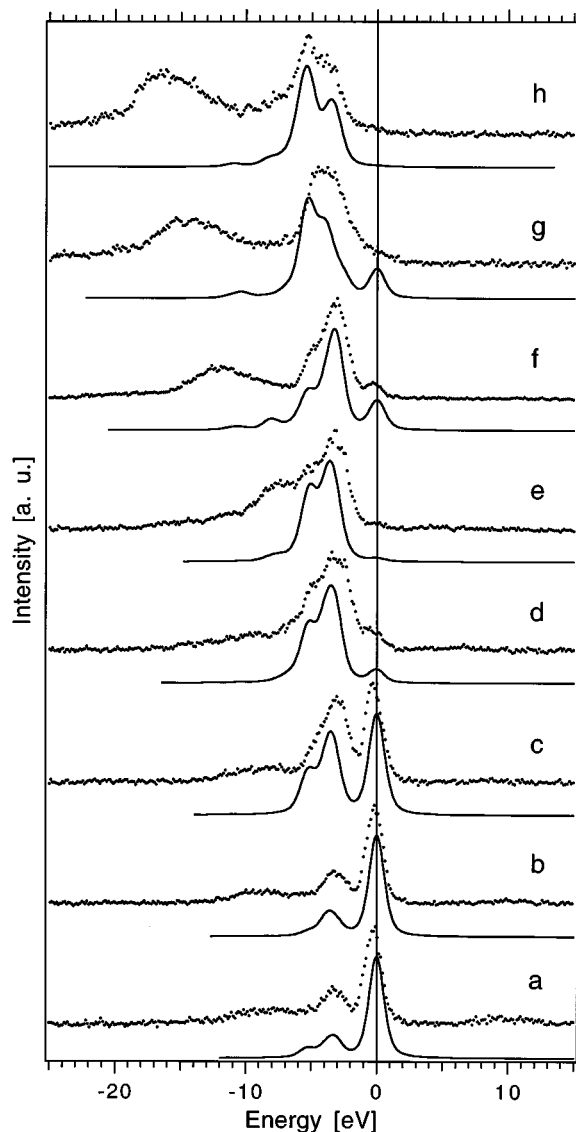


FIG. 2. The resonant x-ray fluorescence spectra (dots) plotted as energy loss spectra relative to the energy of the recombination peak which is set at 0 eV, compared to the calculations for the  $\text{Mn}^{2+}$  ion (solid lines).

is a sufficient approximation in this case as the interference terms are small,<sup>21</sup> because the separation of the  $2p^53d^6$  states of the same symmetry is large compared to the lifetime width.

The atomic multiplet structure and matrix elements of dipole transitions between  $2p^53d^6$  and  $3d^5$  configurations were calculated in intermediate coupling in the spherical  $O_3$  group using Cowan's programs.<sup>22</sup> The radial parts of the  $3d$ - $3d$  Coulomb and  $2p$ - $3d$  Coulomb and exchange multipole interactions (so-called Slater integrals) obtained *ab initio* within the Hartree-Fock limit were scaled down to 80% of their Hartree-Fock values to account for intra-atomic configuration interaction and hybridization effects.

One can see in Fig. 2 that our atomic calculation of the resonant part of the MnO fluorescence spectra is very successful in reproducing the spectra excited on the  $L_3$  multiplet (the spectra *a, b, c, d*). Although the crystal field interaction was neglected, the atomic approach is adequate for the inter-

pretation of experimental data due to an extra stabilization of the  $3d^5$  high-spin configuration by the Hund's rule coupling. Such an exchange stabilization results in a large energy separation between the ground high-spin  $^6S$  and first excited low-spin  $^4G$  states<sup>23</sup> compared to the crystal field splitting. One can see that the main structures in resonant Mn  $L_{\alpha,\beta}$  spectra of MnO appear at about 3 eV below the recombination peak. The separation of this peak from the rest of the multiplet structure is especially pronounced in spectra recorded at the excitation energies labeled by *a* and *b*. The first feature in Fig. 2, spectra *a, b*, on the low-energy side of the recombination peak corresponds to the transitions to the  $^4G$ -,  $^4P$ -, and  $^4D$ -derived states. The  $^4G$ -,  $^4P$ -, and  $^4D$  multiplets themselves are very close to each other in energy,<sup>23</sup> creating a quite compact quadruplet group, so that the energy separation between recombination and the quadruplet-originating peak can be considered as a measure of the exchange interaction. The derived value of the exchange interaction is 3.1 eV which is close to gas phase atomic data for the Mn atom.<sup>19</sup> The main effect of the crystal field splitting is some additional broadening of the spectral features, which does not affect the present analysis.

When the excitation energy is increased in Fig. 2, spectra *c, d*, the loss peak develops a shoulder at a loss energy of about 5 eV. This feature is well reproduced by the calculations. Analysis of the theoretical results shows that this peak is mostly due to final states with  $^2D$ -,  $^2F$ -, and  $^4F$  symmetry. Figure 2, spectra *e* shows that charge-transfer processes play a role, which cannot be reproduced by an atomic calculation.

Spectra from excitation on the  $L_2$  peak are shown in Fig. 2, spectra *f, g, h*. Also here are the experimental *dd* excitation spectra successfully described by the calculations. The intensity of the  $L_{\alpha}$  emission line at the fixed energy of 638 eV (increasing loss energy) can be ascribed to excitations into the  $L_3$  continuum and to Coster-Kronig decay from the  $L_2$  hole states.

A notable success of our calculation is the intensity of the *dd* excitations relative to the recombination line. It shows that our geometry (measuring the emission in the direction perpendicular to the incident beam, in the direction of the linear polarization) suppresses the elastically scattered x rays relative to the two-step process of absorption and reradiation. It is more difficult to calculate the intensity of *dd* excitations in optical spectroscopy or EELS because they are dipole forbidden.

A comparison of experimental fluorescence spectra of MnO with the results of the atomic multiplet calculations also allows one to discriminate the charge-transfer satellites and the contribution of the nonresonant fluorescence in these spectra. The satellites due to charge-transfer excitations ( $3d^6\bar{L}$  where  $\bar{L}$  stands for a hole in the O  $2p$  band) most clearly appear in spectra recorded at the excitation energies *a-d* as weak continuous states with an energy spread over the range of more than 5 eV on the low-energy side of the spectra. It is worth mentioning that a simulation of these fluorescence spectra within the Anderson impurity model can give "true," not renormalized, values for model parameters in the ground state. These parameters are usually derived from the analysis of core-level x-ray photoemission and x-ray absorption data, although it is *a priori* expected that the

hybridization  $V$  and the on-site Coulomb interaction  $U_{dd}$  are different in the presence of a core hole.<sup>24</sup>

In conclusion, we demonstrated the potential of resonant x-ray fluorescence spectroscopy in studies of low-energy excitations using the example of MnO. Due to elemental selectivity and dipole selection rules, the Mn  $3d$  component in the valence band of this oxide is studied separately from other states. By setting the excitation energy near the Mn  $2p$  threshold, the lowest and different excited states of the  $3d^5$  configuration as well as charge-transfer excited states of the  $3d^6L$  configuration are probed as a result of the deexcitation process. The  $dd$  excited loss features are intense in comparison with the recombination peak, because they are optically

allowed. This makes it straightforward to calculate these spectra quantitatively, as shown by the success of an atomic approximation. All these factors make x-ray fluorescence spectroscopy on the  $2p$  resonance of transition metal compounds a potentially powerful tool to measure  $dd$  excitations and ligand-field strengths in mixed and dilute systems.

This work was supported by the Swedish Natural Science Research Council and the Göran Gustavsson Foundation for Research in Natural Sciences and Medicine. The experiments at ALS were also supported by the U.S. Department of Energy, under Contract No. DE-AC03-76SF00098.

\*Present address: MAX-lab, University of Lund, Box 118, S-221 00 Lund, Sweden. On leave from the Institute of Metal Physics, Yekaterinburg, Russia.

<sup>1</sup>W. Schulke, A. Berthold, and A. Kaprolat, *Phys. Rev. Lett.* **60**, 2217 (1988).

<sup>2</sup>F. Sette *et al.*, *Phys. Rev. Lett.* **75**, 850 (1995).

<sup>3</sup>T. Åberg and B. Crasemann, in *Resonant Anomalous X-Ray Scattering*, edited by G. Materlik *et al.* (North-Holland, Amsterdam, 1994), p. 431

<sup>4</sup>F. Gel'mukhanov and H. Ågren, *Phys. Rev. B* **49**, 4378 (1994).

<sup>5</sup>Y. Ma *et al.*, *Phys. Rev. Lett.* **69**, 2598 (1992).

<sup>6</sup>P. W. Anderson, *Phys. Rev.* **115**, 2 (1959).

<sup>7</sup>A. Gorschlüter and H. Merz, *Phys. Rev. B* **49**, 17 293 (1994).

<sup>8</sup>N. Wassdahl *et al.*, in *X-ray and Inner-Shell Processes*, edited by T. A. Carlsson, M. O. Krause, and S. T. Manson, AIP Conf. Proc. No. 215 (AIP, New York, 1990), p. 451.

<sup>9</sup>S. M. Butorin *et al.*, *J. Alloys Compounds* **225**, 230 (1995).

<sup>10</sup>H. A. Padmore and T. Warwick, *J. Synchrotron Radiat.* **1**, 27 (1994), and references therein.

<sup>11</sup>J. Nordgren *et al.*, *Rev. Sci. Instrum.* **60**, 1690 (1989).

<sup>12</sup>J. A. Bearden, *Rev. Mod. Phys.* **39**, 78 (1967).

<sup>13</sup>H. Kurata and C. Colliex, *Phys. Rev. B* **48**, 2102 (1993).

<sup>14</sup>F. M. F. de Groot, *J. Electron Spectrosc.* **67**, 529 (1994).

<sup>15</sup>P. Kuiper *et al.*, *Phys. Rev. Lett.* **70**, 1549 (1993).

<sup>16</sup>G. van der Laan and I. W. Kirkman, *J. Phys.* **4**, 4189 (1992).

<sup>17</sup>U. Arp *et al.*, *J. Phys. B* **25**, 3747 (1992).

<sup>18</sup>B. T. Thole and G. van der Laan, *Phys. Rev. B* **38**, 3158 (1988).

<sup>19</sup>J. Sugar and C. Corlis, *J. Phys. Chem. Ref. Data* **14**, Suppl. 2 (1985).

<sup>20</sup>S.-P. Jeng and V. E. Henrich, *Solid State Commun.* **82**, 879 (1992).

<sup>21</sup>F. M. F. de Groot *et al.*, *Solid State Commun.* **92**, 991 (1994).

<sup>22</sup>R. D. Cowan, *The Theory of Atomic Structure and Spectra* (University of California Press, Berkeley, 1981).

<sup>23</sup>D. van der Marel *et al.*, *Phys. Rev. B* **31**, 1936 (1985).

<sup>24</sup>O. Gunnarsson and O. Jepsen, *Phys. Rev. B* **38**, 3568 (1988); O. Gunnarsson *et al.*, *ibid.* **39**, 1708 (1989); O. Gunnarsson and K. Schönhammer, *ibid.* **40**, 4160 (1989).